Design of an Integrated Modular Motor Drive

Mesut Uğur[1], Ozan Keysan[2]

[1]Middle East Technical University, Ankara, Turkey
ugurm@metu.edu.tr
[2] Middle East Technical University, Ankara, Turkey
keysan@metu.edu.tr

Abstract

In this study, design of an Integrated Modular Motor Drive (IMMD) is performed. The design is based on a modular fractional slot concentrated winding permanent magnet synchronous machine (FSCW-PMSM) and power stage with gallium nitride (GaN) power field effect transistors (FETs). Suitable slot/pole combination and winding configuration are obtained to maximize the stator winding factor as well as reduce the space harmonics on the modular motor. Optimum selection of number of series and parallel motor drive modules is achieved and power device selection is performed based on loss characterization. The performance of the system is obtained with Ansys/Maxwell for the motor and with MATLAB/Simulink for the power stage. The efficiency of the motor drive is enhanced by 2% compared to a conventional motor drive power stage. Power density values larger than 15 W/cm^3 has been achieved which is not attainable with conventional motor drive systems.

1. Introduction

In conventional motor drive systems, the drive units are placed in separate cabinets which increases the overall weight and volume of the system and decreases the power density of the system. Furthermore, the drive units are connected to the motor by means of long cables which causes transient voltage overshoots due to the high frequency pulse width modulation (PWM) operation.

A novel concept called Integrated Modular Motor Drives (IMMDs) has been proposed in the last few years suggesting that all the components of the motor drive system can be integrated onto the motor including power electronics, control electronics, passive components and heat sink (ref). By doing so, the power density of the system can be enhanced significantly which is very critical in aerospace and electric traction applications (ref). In addition to that, cost reduction up to 20% is possible thanks to the elimination of enclosures and connection equipment (ref). Moreover, the absence of connection cables yields less leakage current on the winding insulation which will extend the lifespan of the motor as well as minimize electromagnetic interference (EMI) problems (ref).

In addition, the overall system is segmented with modules sharing the total power equally. By this way, the fault tolerance of the system is increased (ref). The current and voltage ratings of the power semiconductor devices can also be decreased by modularization. Moreover, the components which produce heat due to power loss are spread and distributed in a wider surface area which makes the thermal design more convenient as well as decreases the possible of hot spot formation (ref). Finally, the manufacturing, installation and maintenance costs are considered to decrease thanks to the modular structure (ref).

Integration of the motor and drive also brings several challenges. Firstly, fitting all the drive components to the available space requires size optimization and careful layout design (ref). Second, it is difficult to cool the motor and drive simultaneously since they both produce heat (ref). Furthermore, all the electronic components are subjected to a higher ambient temperature and continuous vibration and should be selected accordingly (ref).

To overcome these challenges, it has been proposed in the literature that wide band gap (WBG) power semiconductor devices such as Gallium Nitride (GaN) can be used which are capable of operating at high frequencies (ref). By doing so, the size of the passive components can be reduced as well as the size of the heat sink thanks to superior efficiency values (ref). On the other hand, high frequency operation highlights the parasitic components on the power stage and gate drive circuits which makes layout design critical (ref).

In this paper, design of an IMMD system is presented with enhanced power density, increased efficiency and enhanced fault tolerance capability. In Section 2, basic structure and current technology prospects of IMMDs are introduced. In section 3, design of the system including the motor and the drive is explained. In section 4, simulation results are presented and in section 5, conclusions are given.

2. Basic Structure of IMMD

There are several types of integration of the motor drive onto the motor. In this paper, integration into the stator back iron is considered, which also allows the modularization of the system. In this configuration, one module is composed of a stator pole piece, a concentrated coil and a power converter dedicated to its own winding along with its controller. Examples of such a structure can be seen in Fig. 1 (ref).

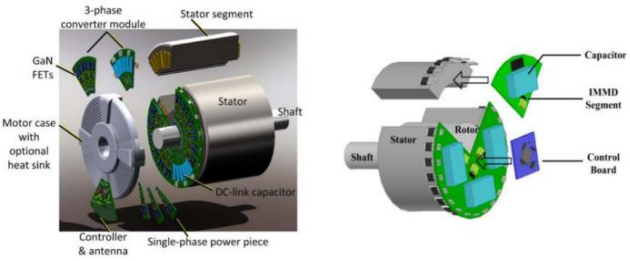

Fig. 1. IMMDs with stator back-iron integration (ref)

Each stator winding belonging to different pole pairs on the stator are usually connected in series to form one phase of the stator in conventional motors. On the other hand, the windings in

different poles can be connected to separate motor drive units in modular motors. These types of motors are also called split-winding motors (ref) and the redundancy and fault tolerance of the system is enhanced thanks to this modularization. Moreover, the motor drive modules can be connected with different configurations which makes the design more flexible.

A general block diagram of one module of an IMMD system is shown in Fig. 2 (ref). On the machine pole, concentrated windings are preferred for their easy manufacturing and suitability for split-winding stators, especially in modular motors. Fractional slot concentrated winding (FSCW) permanent magnet synchronous motors (PMSMs) are very common in IMMD studies thanks to their high power density, high torque density, low cogging torque and good fault tolerance capability (ref).

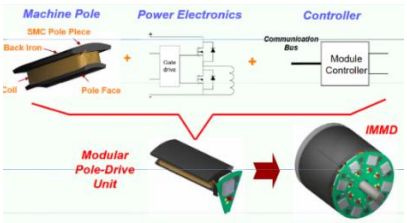

Fig. 2. General block diagram of one module of an IMMD (ref)

As for the power electronics, many different topologies have been proposed for AC motor drive systems such as, two-level inverter, multilevel neutral point clamped inverter, multilayer flying capacitor inverter, inverter with high frequency transformer etc. (ref). As mentioned previously, for a modular motor drive, several other motor drive topologies become available thanks to the design flexibility. Furthermore, the aforementioned topologies can be connected in series and/or parallel on the DC link to form a new topology. Series and parallel connection of motor drive inverter modules on the DC link are shown in Fig. 3 alongside with a conventional motor drive (ref). These types of connections are possible due to the fact that the windings, which are split and hence electrically isolated, do not cause circulating currents among the inverter modules. The major advantage of this possibility is to be able to split the voltage and/or current requirement of each inverter. One practical usage of this fact is the availability of low voltage power semiconductor device utilization such as GaN in case of high DC link voltage.

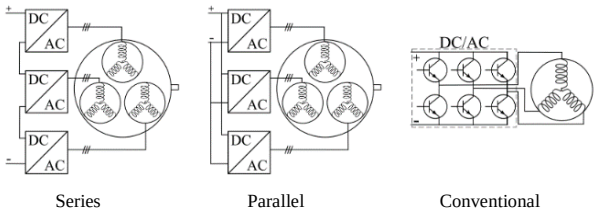

Fig. 3. Different motor drive inverter connections for a modular motor (ref)

The employability of GaN devices is especially crucial for IMMD systems because these devices are one of the so-called WBG type semiconductor devices. These devices have much higher switching speeds compared to conventional silicon based devices such as Insulated Gate Bipolar Transistors (IGBTs) and admissible on-state losses which make them very efficient [ref]. Moreover, they have higher maximum junction temperatures [ref]. The volume reduction challenge of IMMDs can be addressed by the utilization of GaNs thanks to higher efficiency which makes cooling easier, and their fast switching speed which enables high switching frequencies reducing the size of passive components. In high power applications, the maximum switching frequency which can be applied to an IGBT is limited to 20 kHz, whereas GaNs can be used with frequencies as high as 100 kHz in applications with kW range [ref]. Another reason is that the efficiency of the system is high not only in rated power, but also for a wide range of output power [ref]. As a matter of fact, GaNs have been utilized in most of the very first IMMD prototypes thanks to these reasons [ref].

3. Design of the IMMD System

The design process of the IMMD system can be considered in twofold: design of the motor and design of the drive. However, they should be considered simultaneously for an integrated system as one side effects the other significantly. The first assumption in the design process is that the motor drive input is a passive diode bridge rectifier with an LC DC link filter. The effects of this rectifier module on the rest of the system are kept out of the scope of this study such that the input to the motor drive DC link is a pure DC current. The machine is a three-phase permanent magnet synchronous machine having a modular stator with fractional slot concentrated windings. Considering the applications where IMMD concept is suitable, it will be a low speed high torque motor design. The system parameters used in the design process are shown in Table 1.

The first parameters to be decided for the design is the total number of three-phase modules. As stated before, the number of series or parallel connected modules can be varied according to the voltage and current requirements and the system parameters such as the DC link voltage and total output power. It has also been specified that GaN transistors should be used to reach the efficiency ratings and meet the volume reduction challenge. Blocking voltage rating of the current GaN transistors which are commercially available is 650V at most [ref]. If two-level full-bridge motor drive inverter modules are used, the minimum power semiconductor blocking voltage rating in this design is 810V. This value is calculated based on a safety margin considering the voltage overshoot effects due to parasitic inductances and high switching speed. It is clear that, at least two series modules should be used with the aforementioned GaN devices. This also makes the total number of modules an even number.

Table 1. The system parameters used in IMMD design process

DC link voltage, V_{dc}	540 V
Total output power, P_{out}	8 kW
Motor efficiency aim, $\eta_{m,a}$	96%
Drive efficiency aim, $\eta_{d,a}$	98%
Rated speed, N_r	600 rpm

There are various parameters which effect the number of parallel modules. One of them is the required power rating of each module which effect the current ratings of the semiconductor devices and drive efficiency. Another one is the number of stator slots. Instead of number of slots per pole per phase (q) used in conventional systems, a new parameter, number of slots per module per phase (w) should be defined in IMMDs. For example, if two series and two parallel modules are used, the minimum number of slots that can be used is 24. Lastly, the effect of interleaving and its utilization for minimization of DC link

capacitor bank size is considered to determine the number of modules. In [ref-u], the effect of the number of modules and applied interleaving angle to the current ripple on the DC link capacitor bank is studied for an IMMD system, and it has been shown that selecting four modules yields best results in terms of DC link capacitor size. Using that result, it is decided that a total number of 4 modules which are 2-series and 2-paralel should be used. The schematic diagram of the suggested IMMD system topology is shown in Fig. 4.

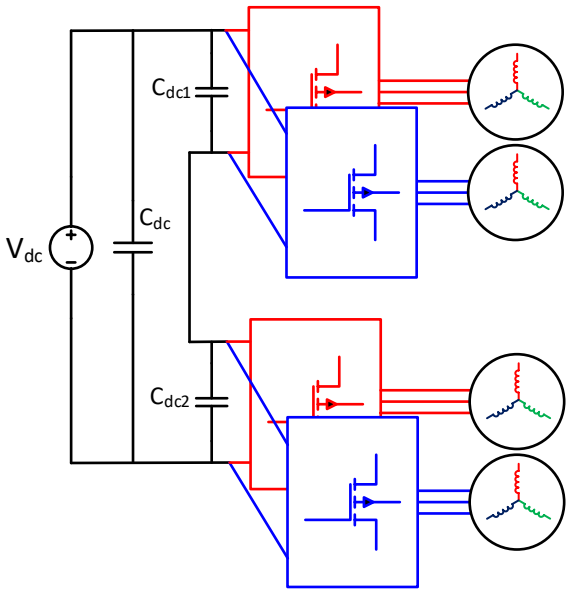

Fig. 4. Schematic diagram of the suggested IMMD topology

3.1. Design of the motor

The main dimensions of the motor are determined by using the torque requirement, magnetic loading (B) and electrical loading (A) selected for the IMMD application, as shown in Equation X. V stands for the volume which is shown in Equation Y, where D is the bore diameter and L is the axial length of the motor. The aspect ratio, which is the ratio of the diameter to the length is selected as 0.3 for this application. The outer diameter is decided using a few iterations considering the magneto motive force drop across the back iron. The number of slots should be an integer multiple of 24 since the number of 3-phase modules is 4. For the given dimensions, 48 slots yield better results. Moreover, the number of rotor poles is found according to fundamental winding factor.

The number of turns per coil side can be determined by the induced voltage requirement of each phase of each module, which can be expressed as in Equation 1, in rms, where $N_{ph\text{-}m}$ is number of turns per phase per module, f is the applied fundamental frequency at rated conditions, Φ_{pp} is the flux under a pole and k_w is the fundamental winding factor. The flux per pole can be calculated using the machine dimensions and air gap flux density (B_g) as in Equation 2, where D_{is} is the bore diameter, L is the axial length, and p is the number of poles. The winding factor is determined using the pre-calculated tables created for fractional slot machines in terms of slot/pole combinations as 0.933. The fundamental frequency is also determined by the rated speed and pole number of the synchronous motor, as in Z. Assuming that the motor drive inverters are switched with sinusoidal pulse width modulation (SPWM) technique, the terminal voltage of one phase of each module is determined using T. The required number of turns per coil side is found using this equation as ccc.

The resultant motor parameters are shown in Table 2. In Figure 5, the proposed 2-layer winding diagram of one module is shown. The main purpose of this diagram is having large enough winding factor while keeping the harmonic content low.

$$T = V\,B\,A \quad \text{(X)}$$

$$V = \pi\,D^2\,L\,/\,4 \quad \text{(Y)}$$

$$E_{ph\text{-}m} = 4.44\,N_{ph\text{-}m}\,f\,\Phi_{pp}\,k_w \quad (1)$$

$$\Phi_{pp} = 2\,D_{is}\,L\,B_g\,/\,p \quad (1)$$

$$f = N_m\,p\,/\,120 \quad (1)$$

$$V_{ph\text{-}m} = m_a\,V_{dc\text{-}m}\,/\,2\sqrt{2} \quad (1)$$

$$z_Q = 2\,N_{ph\text{-}m}\,/\,w\,l \quad (1)$$

Table 2. The resultant motor parameters

Number of stator slots, Q_s	24
Number of rotor poles, p	20
Stator winding factor, k_{ws}	0.933
Motor axial length, L	150 mm
Stator outer diameter, D_{os}	230 mm
Stator inner diameter, D_{is}	150 mm
Air gap length, l_g	1 mm
Magnet thickness, l_m	5 mm
Number of turns per coil side, z_Q	30
Stator fill factor, k_{cu}	0.6

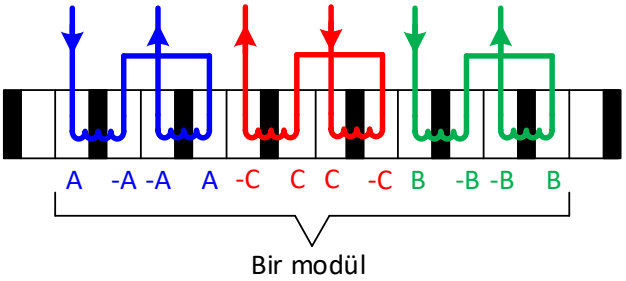

Fig. 5. Proposed winding diagram of one module

3.2. Design of the drive

The selection of power semiconductor device is based on voltage and current requirements. Among the suitable alternatives, the final selection is based on drive efficiency. The voltage requirement of each device is already established. There are two GaN transistor types in the market which have breakdown voltage ratings as high as 650V, cascade GaNs manufactured by Transphorm and enhancement mode (e-mode) GaNs manufactured by GaN systems [ref]. The next step is to determine the current requirement. By using the phase voltage calculated in the previous step, the phase current of each module can be found by using X as Y A.

$$I_{ph\text{-}m} = P_{out\text{-}m}\,/\,3\,\eta_m\,cos(\Phi)\,f\,V_{ph\text{-}m} \quad (1)$$

One device from each type is selected having similar ratings as well as an IGBT for comparison purposes, which are shown in Table X [ref]. Power semiconductor device losses can be categorized as forward conduction loss (P_{tc}), transistor switching loss (P_{ts}), reverse conduction loss (anti-parallel diode loss for IGBTs, P_{dc}) and reverse recovery loss (P_{dr}). The equations used in the loss calculations are shown in X-Y. An approximate method well-established and commonly used for moor drive inverters is utilized in these equations for simplicity. In these equations, E_{on} and E_{off} stand for turn-on and turn-off energies, V_{ce-sat} is saturation voltage drop for the IGBT, R_{ds-on} is the on-state resistance for GaN, V_{ec} is the reverse voltage drop, I_{rr} and trr are the diode reverse recovery current and time, respectively, and V_{ce-p} is the reverse recovery peak voltage.

$$P_{tc} = I_{cp}\, V_{ce,sat} \left(\frac{1}{8} + \frac{M\, pf}{3\,\pi}\right) \quad (IGBT) \tag{7}$$

$$P_{tc} = {I_{cp}}^2\, R_{ds,on} \left(\frac{1}{8} + \frac{M\, pf}{3\,\pi}\right) \quad (GaN) \tag{8}$$

$$P_{ts} = \left(E_{on} + E_{off}\right) \frac{f_{sw}}{\pi} \tag{9}$$

$$P_{dc} = I_{ep}\, V_{ec} \left(\frac{1}{8} - \frac{M\, pf}{3\,\pi}\right) \tag{10}$$

$$P_{dr} = I_{rr}\, t_{rr} V_{ce,p}\, \frac{f_{sw}}{8} \tag{11}$$

Table X. Alternative devices for transistor selection [ref]

Transistör	FP35R12KT4P	TPH3205WSB	GS66508B
Tipi	IGBT	Cascode GaN	E-mode GaN
Üretici	Infineon	Transphorm	GaN systems
Gerilim	1200 V	650 V	650 V
Akım	35 A	35 A	30 A
$V_{ce,sat}$	2,15 V	-	-
$R_{ds,on}$	-	60 mΩ	50 mΩ

4. Simulation Results

The performance of the motor is analyzed using Ansys/Maxwell simulation environment. The analytical results are shown in Table Y. The designed motor is simulated using 2D FEM analysis tool to obtain magnetostatic and transient results. The magnetic flux density

Table X. Alternative devices for transistor selection [ref]

Transistör	FP35R12KT4P	TPH3205WSB	GS66508B
Tipi	IGBT	Cascode GaN	E-mode GaN
Üretici	Infineon	Transphorm	GaN systems
Gerilim	1200 V	650 V	650 V
Akım	35 A	35 A	30 A
$V_{ce,sat}$	2,15 V	-	-
$R_{ds,on}$	-	60 mΩ	50 mΩ

Equations

Konvansiyonel IGBT'li motor sürücü ile iki farklı tipte GaN'lı TMMS sistemi kayıp analizi karşılaştırmalı sonuçları Şekil 6'da gösterilmiştir.

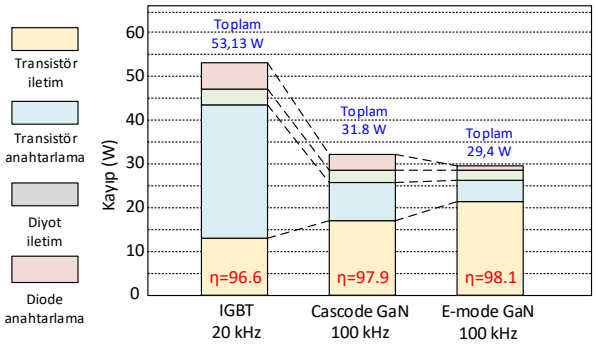

Şekil 6. Konvansiyonel motor sürücü sistemi ile TMMS sistemi kayıp analizi sonuçları

Kayıp analizi sonuçlarına bakıldığında GaN kullanımı ile her iki tipte de anahtarlama frekansı beş katına çıkartılmasına rağmen yarıiletken kayıplarının toplamda hemen hemen yarıya düştüğü gözlenmiştir. IGBT'lerde pratikte anahtarlama frekansı üst sınırı 20 kHz'tir, bu nedenle daha yüksek frekanslarda analiz yapılmamıştır. Kayıp bileşenleri ayrı ayrı incelendiğinde ise, öngörüldüğü gibi kayıptaki ana düşüş transistor ve diyot anahtarlama kayıplarında olmaktadır. Diğer bir taraftan, diyot iletim kayıplarında büyük bir değişim gözlenmemiştir ancak transistor iletim kayıpları GaN'larda daha yüksek olmuştur. Bu durumun başlıca nedenleri, IGBT'lerin yüksek akımlı uygulamalarda iletim durumunda genel olarak iyi performans göstermesi ve GaN gibi WBG anahtarların henüz teknolojik olarak istenilen iletim durumu düzeyine ulaşamamasıdır. Diğer bir neden ise sistemin iki paralel ve iki seri modülden oluşmasıdır. Tamamının paralel bağlanmasına durumuna oranla her bir modül iki kat fazla akım taşımakta ve GaN'larda iletim kayıpları akımın karesi ile artmaktadır. Sonuç olarak, 100 kHz anahtarlama frekansında hem Kaskod hem de E-mode GaN'da yaklaşık %98 verime ulaşılmıştır ve daha yüksek verim hedeflendiğinde anahtarlama frekansı düşürülebilir.

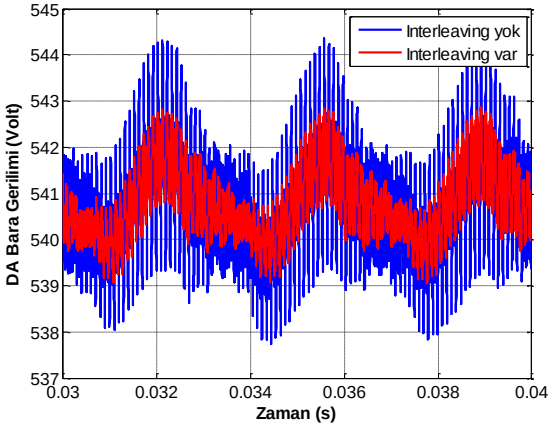

Şekil 7. DA bara gerilimi dalgalanması

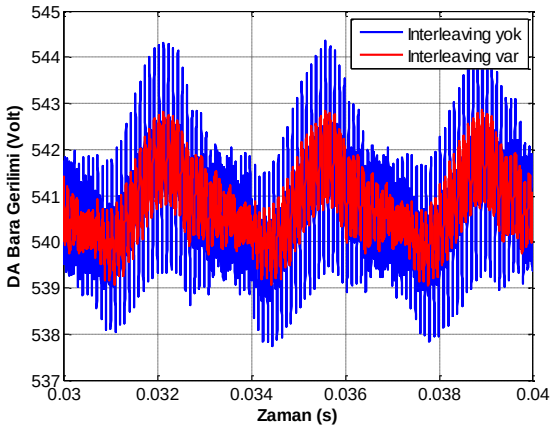

Şekil 7. DA bara gerilimi dalgalanması

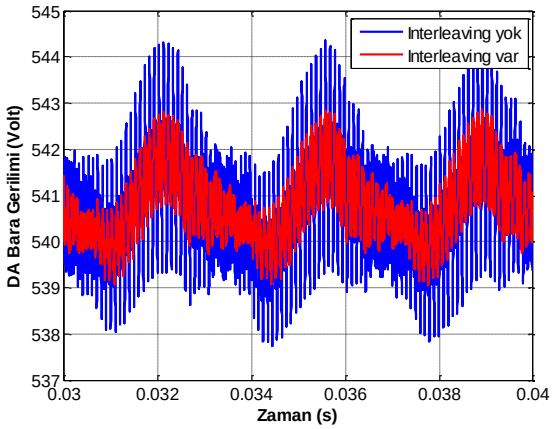

Şekil 7. DA bara gerilimi dalgalanması

5. Conclusions

Define abbreviations and

6. References

[1] J. K. Author, "Name of paper", *Abbrev. Title of Periodical*, vol. *x*, no. *x*, pp. *x-x*, Abbrev. Month, year.

[2] J. K. Author, "Title of book", Abbrev. of Publisher, City of Publisher, Country, year.

[3] J. K. Author, "Title of paper", in *Unabbreviated Name of Conf.*, City of Conf., Abbrev. State (if given), year, pp. *x-x*.

[4] J. K. Author, "Title of thesis", M.S. thesis, Abbrev. Dept., Abbrev. Univ., City of Univ., Abbrev. State, year.

[5] *Title of Standard*, Standard number, date.

[6] J. K. Author. (year, month day). *Title* (edition) [Type of medium]. Available: http://www.(URL)